*Mathematical Biosciences and Engineering*

https://www.aimspress.com/journal/mbe

MBE, 22(11): 2852–2869.
DOI: 10.3934/mbe.2025105
Received: 03 April 2025
Revised: 21 July 2025
Accepted: 01 September 2025
Published: 15 September 2025

*Research article*

# Quantitative analysis of respiratory viral triple infections: Examining within host dynamics of Influenza, RSV, and SARS-CoV-2

**Saanvi Srivastava and Hana M. Dobrovolny***

Department of Physics & Astronomy, Texas Christian University, 2800 S. University Drive, Fort Worth, TX 76109, USA

* **Correspondence:** Email: h.dobrovolny@tcu.edu

**Abstract:** Prior research has explored co-infections that involve two respiratory viruses, yet triple infections remain poorly elucidated. With the COVID-19 pandemic and seasonal epidemics of respiratory syncytial virus (RSV) and influenza, understanding the dynamics of triple infections is critical for public health preparedness. The simultaneous circulation of influenza A virus (IAV), RSV, and SARS-CoV-2 presents a significant public health burden, particularly among vulnerable populations such as children, the elderly, and immunocompromised individuals. Comprehending the interactions among these viruses is crucial to improve our capacity to forecast and curb disease outbreaks. This study addresses the escalating concern over the interaction of multiple respiratory viruses by introducing a simple mathematical model to analyze triple infection dynamics involving IAV, RSV, and SARS-CoV-2. The central question addressed in this study is how variations in infection rates influence each virus's duration and peak viral load in a triple-infection scenario. We find distinct regimes where each virus can dominate and suppress the viral load and duration of the remaining two viruses. We derive an analytical expression for the dependence of the critical infection rate of one virus on the infection rates of the other two viruses. While the model will need to be extended to realistically capture in vivo viral dynamics, this analysis helps provide insight into the complex dynamics of multiple virus infections.

**Keywords:** viral infection; infection rate; mathematical model; respiratory virus; coinfection

## 1. Introduction

Viruses pose significant health risks due to the potential for complications in affected individuals. Viruses often co-circulate within populations, which creates opportunities for simultaneous infections [1–3]. This co-circulation can lead to complex interactions among viruses, potentially exacerbating the severity of illness [4, 5]. Public health authorities are particularly concerned about the potential for a tripledemic of influenza A virus (IAV), respiratory syncytial virus (RSV), and SARS-CoV-2 [5–7],

with work being done to improve the tests for multiple pathogens [8–11] and to examine possible treatment and prevention options [12, 13].

Within a host, viruses are known to interact through mechanisms such as competition for cellular resources [14, 15], modulation of the immune response [16–18], and synergistic effects on disease progression [17, 19, 20], which leads to more severe disease outcomes [21, 22]. For instance, viral interference, where one virus affects the replication of another, has been observed in co-infections involving IAV and RSV, although with mixed results. Some studies suggest that IAV can suppress RSV replication under certain conditions [23–25], although other studies suggest that RSV infection can also block IAV [26, 27]. Additionally, both RSV [28, 29] and IAV [29–32] have also been shown to block SARS-CoV-2 infections. However, other studies indicate instances of viral synergy, with IAV and SARS-CoV-2 co-infections leading to more severe outcomes [17, 20, 21, 33].

These complex interactions necessitate a deeper understanding of how viruses coexist and compete in within-host environments. Infections with multiple pathogens are not only theoretically significant but have also been documented in various clinical contexts [34, 35]. Notably, recent studies revealed that the number of patients with 3 or more respiratory pathogens is about 2–4% [1, 36–38]. This can significantly increase the risk of hospitalization and severe disease outcomes, especially in vulnerable populations such as young children and the elderly [37]. This underscores the importance of considering viral co-infections during diagnosis and treatment, particularly in high-risk groups and during peak viral seasons.

Mathematical modeling has become an increasingly important tool to help develop our understanding of viral infections [39–41]. In recent years, models have been used to examine the role of the immune response [42, 43], the effect of vaccination [43–45] and antiviral treatment [46–48], along with a variety of other processes such as syncytia formation [49], the bystander effect [50], reinfection [51], and dose-dependence [52]. Mathematical modeling has emerged as a particularly invaluable tool to explore the dynamics of viral interactions. These models have examined the effect of target cell competition [14, 53], cell regeneration [54, 55], super-infection [55], and other viral interactions [53, 56, 57]. Despite these advances, gaps remain in the research, particularly concerning the dynamics of triple infections. One model was developed to examine triple infections [58], although it was only used to examine viral time course for a specific set of parameters. This does not account for the emergence of different SARS-CoV-2 or influenza variants, which have demonstrated altered infectivity [59–61]. These variants raise concerns regarding their impact on triple infections. Studies have indicated that these variants can influence viral load and prolong the duration of illness, underscoring the need for comprehensive models that incorporate variant characteristics to accurately predict co-infection dynamics [62].

In light of these findings, this research seeks to develop a mathematical model that captures the dynamics of triple infections by exploring how variations in infection rates influence the duration and maximum viral load of IAV, RSV, and SARS-CoV-2 in a triple infection scenario. Through simulations, we evaluate the intricate dynamics of these viruses and uncover patterns in their responses to varying transmission rates. We find that only one virus dominates the triple infection, with the dominant virus suppressing replication of the other two viruses.

## 2. Methods

### 2.1. Model description

We use a model that extends a basic co-infection model to include three viruses, each with its set of equations that represent the dynamics of susceptible target cells ($T$), eclipse-phase infected cells ($E_1, E_2, E_3$), productively infectious cells ($I_1, I_2, I_3$), and viral particles ($V_1, V_2, V_3$). The model equations are as follows:

1. Target Cells ($T$):

$$\frac{dT}{dt} = -\beta_1 T V_1 - \beta_2 T V_2 - \beta_3 T V_3$$

2. Eclipse Phase Infected Cells ($E_1, E_2, E_3$):

$$\frac{dE_1}{dt} = \beta_1 T V_1 - k_1 E_1$$

$$\frac{dE_2}{dt} = \beta_2 T V_2 - k_2 E_2$$

$$\frac{dE_3}{dt} = \beta_3 T V_3 - k_3 E_3$$

3. Productively Infectious Cells ($I_1, I_2, I_3$):

$$\frac{dI_1}{dt} = k_1 E_1 - \delta_1 I_1$$

$$\frac{dI_2}{dt} = k_2 E_2 - \delta_2 I_2$$

$$\frac{dI_3}{dt} = k_3 E_3 - \delta_3 I_3$$

4. Viral Particles ($V_1, V_2, V_3$):

$$\frac{dV_1}{dt} = p_1 I_1 - c_1 V_1$$

$$\frac{dV_2}{dt} = p_2 I_2 - c_2 V_2$$

$$\frac{dV_3}{dt} = p_3 I_3 - c_3 V_3.$$

For these equations, $\beta_1, \beta_2, \beta_3$ represent the viral infection rates, $k_1, k_2, k_3$ represent the transition rates from eclipse phase to productive infection, $\delta_1, \delta_2, \delta_3$ represent the death rates of infectious cells, $p_1, p_2, p_3$ represent the viral production rates, and $c_1, c_2, c_3$ represent the viral clearance rates.

**Table 1.** Model parameters taken from [14] and [63].

| | |
|---|---|
| **Initial Conditions** | |
| $T_0$ | 1.0 |
| $E_{i0}$ | 0 |
| $I_{i0}$ | 0 |
| $V_{i0}$ | 1.0 (PFU/mL) |
| **Viral Infection Parameters** | |
| $\beta_{\text{IAV}}$ | $8.273 \times 10^{-6}$ (PFU/mL$^{-1} \cdot$ day$^{-1}$) |
| $\beta_{\text{RSV}}$ | 0.03 (PFU/mL$^{-1} \cdot$ day$^{-1}$) |
| $\beta_{\text{SARS}}$ | $2.32 \times 10^{-4}$ (PFU/mL$^{-1} \cdot$ day$^{-1}$) |
| **Transition Rates** | |
| $k_{\text{IAV}}$ | 4.20 (day$^{-1}$) |
| $k_{\text{RSV}}$ | 1.27 (day$^{-1}$) |
| $k_{\text{SARS}}$ | 4.08 (day$^{-1}$) |
| **Death Rates** | |
| $\delta_{\text{IAV}}$ | 4.20 (day$^{-1}$) |
| $\delta_{\text{RSV}}$ | 1.27 (day$^{-1}$) |
| $\delta_{\text{SARS}}$ | 38.1 (day$^{-1}$) |
| **Viral Production Rates** | |
| $p_{\text{IAV}}$ | $0.12 \times 10^9$ (PFU/mL $\cdot$ day$^{-1}$) |
| $p_{\text{RSV}}$ | $76.45 \times 10^2$ (PFU/mL $\cdot$ day$^{-1}$) |
| $p_{\text{SARS}}$ | $4.78 \times 10^5$ (PFU/mL $\cdot$ day$^{-1}$) |
| **Viral Clearance Rates** | |
| $c_{\text{IAV}}$ | 4.03 (day$^{-1}$) |
| $c_{\text{RSV}}$ | 1.27 (day$^{-1}$) |
| $c_{\text{SARS}}$ | 0.117 (day$^{-1}$) |

### *2.2. Simulations*

The model uses initial conditions $(T_0, E_{i0}, I_{i0}, V_{i0})$ and parameter values from Table 1 to simulate the triple infection of IAV, RSV, and SARS-CoV-2. The model parameters are taken from fits of a single infection model to IAV, RSV, and SARS-CoV-2 [14, 63]. The infection rates and production rates are scaled so that viral dynamics remain the same when all viruses have the same initial viral inoculum of 1.0 PFU/mL. When the viral measurements change to $V' = V/V_0$, $\beta$ and $p$ must also be converted to the new viral unit with $\beta' = \beta V_0$ and $p' = p/V_0$, respectively. Simulations of the three infections as mono-infections are shown in Figure 1. We see that IAV has a high peak viral load and a short duration. RSV has a low peak viral load and a moderate duration. SARS-CoV-2 has a peak viral load slightly higher than RSV, but a longer duration than both IAV and RSV.

Our approach involves using Python's `scipy.odeint` to numerically solve the system of differential equations that model viral triple infection dynamics. We vary the infection rates and measure two characteristics of the viral titer curve to determine how changes in viral infection rate affect the viral load of the three viruses. We measure the peak viral load and the duration of the infection, which is defined as the time the viral titer curve is above 10 PFU/mL, a typical threshold of detection for

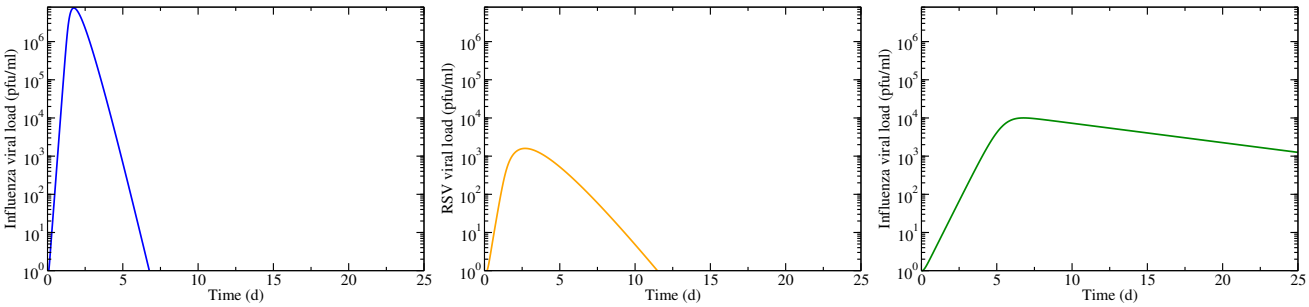


**Figure 1.** Viral load of mono-infections of IAV (left), RSV (center), and SARS-CoV-2 (right).

infectious viral load.

## 3. Results

### *3.1. Model analysis*

Since there is no cell regeneration, there are an infinite number of fixed points $(T^*, 0, 0, 0, 0, 0, 0, 0, 0, 0)$, similar to the coinfection model analyzed in [54]. The presence of an acute infection is determined by the basic reproduction number, which is determined by the next generation matrix method [54],

$$R_0 = \max\left(\frac{\beta_{\text{IAV}} p_{\text{IAV}} T_0}{c_{\text{IAV}}\delta_{\text{IAV}}}, \frac{\beta_{\text{RSV}} p_{\text{RSV}} T_0}{c_{\text{RSV}}\delta_{\text{RSV}}}, \frac{\beta_{\text{SARS}} p_{\text{SARS}} T_0}{c_{\text{SARS}}\delta_{\text{SARS}}}\right). \tag{3.1}$$

Thus there will be an infection if any one of the viruses has an $R_0 > 1$.

### *3.2. Changing infection rate of a single virus*

First, we examine how the triple infection changes when only one of the viruses experiences a change in infectivity. We vary $\beta_i$ from $10^{-3}$ to $10^3$ times its original value and measure the peak viral load and infection duration of all three viruses. The results are shown in Figure 2. The change in infection rate ($\beta_i$), which is displayed on a logarithmic scale, is on the x-axis, while the y-axis denotes the peak viral load (top) and infection duration (bottom). Each line on the graph corresponds to a different virus: IAV (blue), RSV (orange), and SARS-CoV-2 (green).

In the top row, we change $\beta_{\text{IAV}}$; thus, IAV has an infection rate too low to initiate an influenza infection until an infection rate of $\sim 10^{-1.5}$, after which a substantial increase in peak viral load is observed, reaching a maximum at an infection rate of $\sim 10^{0.3}$ with a maximum peak viral load of $\sim 10^{6.75}$. Beyond this point, the virus population stabilizes and maintains a high peak viral load. Contrastingly, the orange line, which represents the peak viral load of RSV, has a maximum peak viral load of $\sim 10^{3.3}$ at low $\beta_{IAV}$. This population remains constant until the IAV viral peak reaches its maximum, after which a gradual decline is evident. The green line, which represents the peak viral load of SARS-CoV-2, shows a similar pattern to RSV, although it has a much lower peak viral load of $\sim 10^{0.9}$. This viral load remains constant until the IAV peak viral load reaches a maximum, after which a decline is observed.

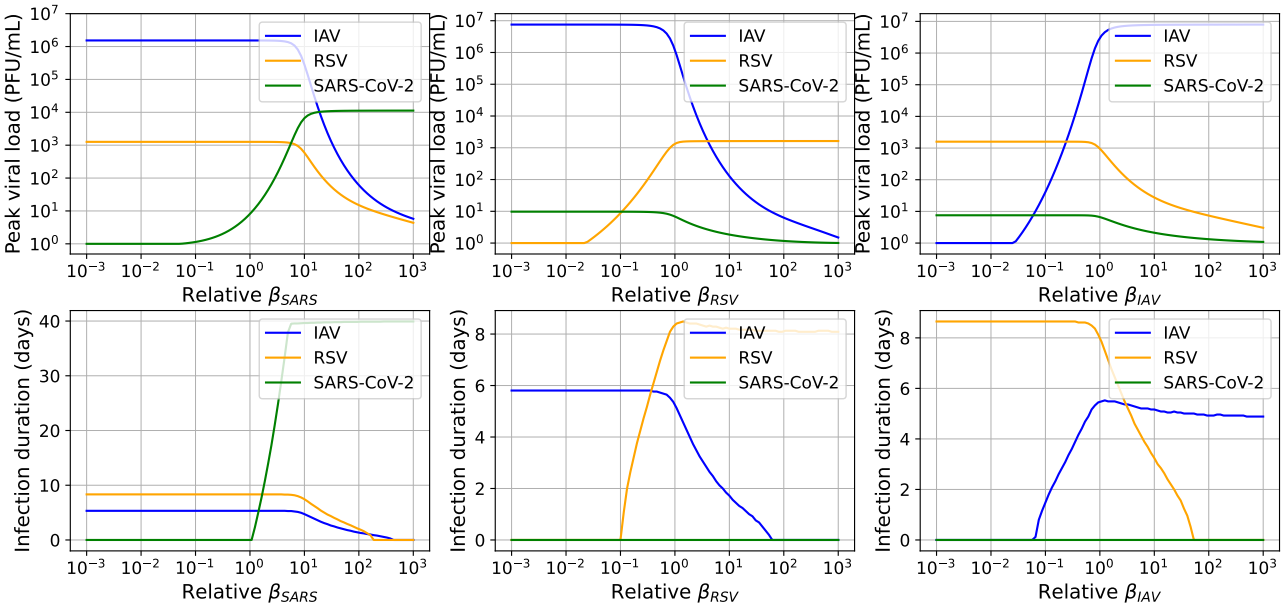


**Figure 2.** Change in peak viral load (top) and infection duration (bottom) for all three viruses as the infection rates of SARS-CoV-2 (left), RSV (center), or IAV (right) are varied.

We see slightly different behaviors for the infection duration. The green line, which represents SARS-CoV-2, never crosses the threshold of detection; thus, SARS-CoV-2 is effectively suppressed by the presence of the other two viruses. On the other hand, RSV has a long duration of around 8.5 d when the infection rate of IAV is low. However, once IAV infections are possible, the duration of RSV steadily declines until $\beta_{\text{IAV}} \approx 10^{1.85}$, where the duration reaches zero and RSV is also effectively suppressed by IAV. IAV duration is zero until an IAV infection rate of $\beta_{\text{IAV}} \approx 10^{-1.2}$ is reached. It subsequently experiences an increase, and peaks at an infection rate of $\sim 10^{0.1}$ with a duration of approximately 5.5 d. The duration slightly decreases at high infection rates since the higher infection rate leads to a more rapid infection of cells, thus a shorter infection duration.

We see similar patterns when changing the infection rate of RSV and SARS-CoV-2. There is a minimum infection rate needed for the associated infection to take hold. Once that particular virus has an infection rate beyond the threshold, the viral peak of the remaining two viruses starts to decrease as the third virus starts to infect the target cells, which leaves fewer cells available for the remaining two viruses. Perhaps the most dramatic shift occurs for SARS-CoV-2, which has a low viral peak and does not rise above the threshold of detection in the presence of other viruses. When the infection rate of SARS-CoV-2 increases, it rises to high viral loads and can suppress both IAV and RSV.

These simulations show that there are critical threshold values for the infection rate of each virus, corresponding to the basic reproduction number for the model (Equation (3.1)). Thus, whether or not a particular virus grows is determined by the $R_0$ derived from single viral infections. Infections will grow if $R_0 > 1$; thus, we can determine the threshold infection rate values for all three viruses by letting $R_0 = 1$, which produces the following:

$$\beta_c = \frac{c\delta}{pT_0}. \tag{3.2}$$

If we assume $T_0 = 1$, we find that IAV needs a minimum infection rate of $1.41\times10^{-7}$ PFU/mL$^{-1}\cdot$day$^{-1}$

or $1.7 \times 10^{-2}\beta_{\text{IAV}}$, RSV needs a minimum infection rate of $2.11\times10^{-4}$ PFU/mL$^{-1}\cdot$day$^{-1}$ or $7.0 \times 10^{-3}\beta_{\text{RSV}}$, and SARS-CoV-2 needs a minimum infection rate of $9.33\times10^{-6}$ PFU/mL$^{-1}\cdot$day$^{-1}$ or $4.22 \times 10^{-2}\beta_{\text{SARS}}$. Note that our simulations show that the threshold infection rate values are slightly higher than the calculated values because the other viruses are infecting the cells, thus the actual available target cells are less than 1.

### *3.3. Changing infection rates of multiple viruses*

In reality, we don't expect that one virus will mutate while the other two remain the same. All three viruses will be mutating at the same time. So what happens when more than one virus undergoes mutations that increase their infection rate at the same time? To investigate this possibility, we examined the effect of changing the infection rate for more than one virus at a time. The results are shown in Figures 3, 4, and 5. The top row of each figure shows the peak viral load for IAV (left), RSV (center), and SARS-CoV-2 (right) while the bottom row shows the corresponding infection durations as the different combinations of viral infection rates are changed. Figure 3 shows the results when IAV and RSV infection rates are changed. Figure 4 shows the results when IAV and SARS-CoV-2 infection rates are changed. Figure 5 shows the results when the RSV and SARS-CoV-2 infection rates are changed.

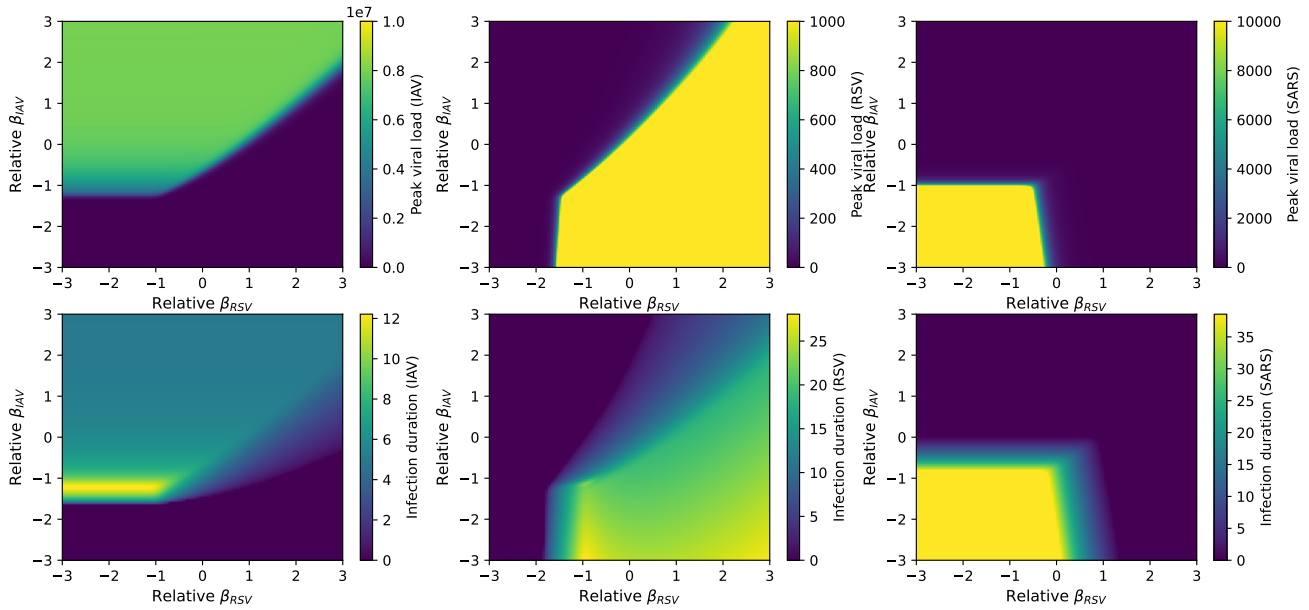


**Figure 3.** Peak viral load (top row) and infection duration (bottom row) for IAV (left), RSV (center), and SARS-CoV-2 (right) while changing the relative infection rates for IAV and RSV. Yellow indicates either high peak viral loads or long infection durations, while dark blue indicates no infection.

Consistent with the simulations that only change one infection rate, we see fairly abrupt changes in peak viral load, which transition from no infection to a high peak viral load at specific values for the infection rate. Of perhaps more interest are the two figures where we see little or no change in the peak viral load as the infection rates change. In Figure 4, the peak viral load of RSV only decreases when the IAV infection rate is very high. In Figure 5, the peak viral load of IAV does not change at all when the infection rates of the other two viruses are varied. This indicates that neither the RSV nor

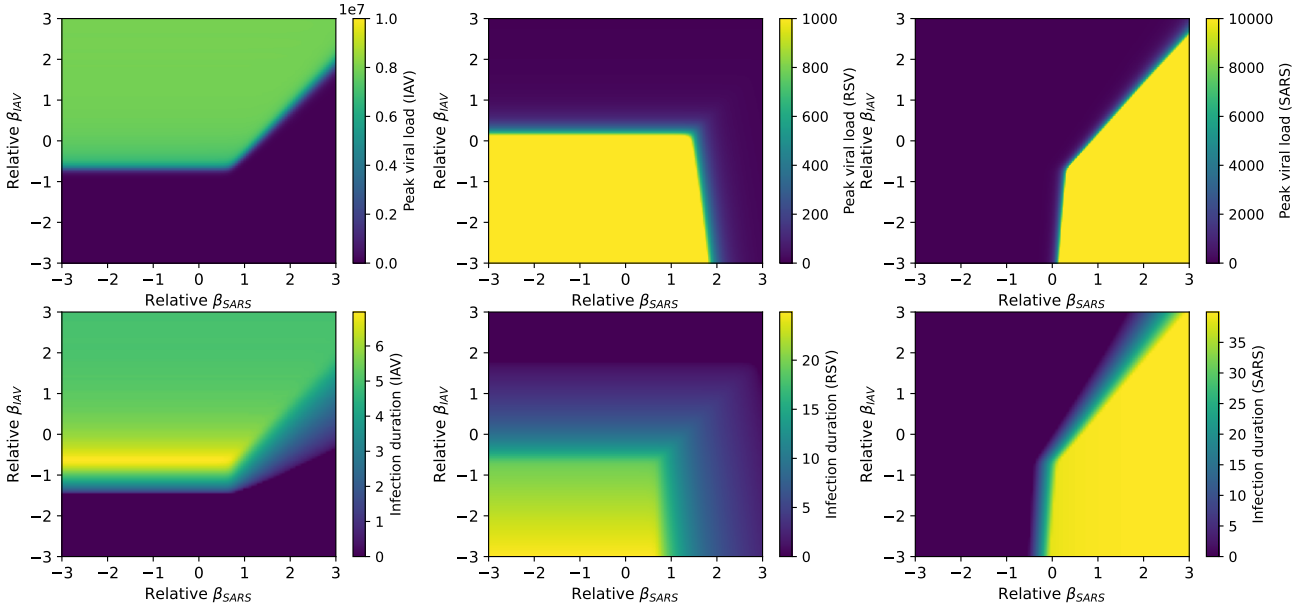


**Figure 4.** Peak viral load (top row) and infection duration (bottom row) for IAV (left), RSV (center), and SARS-CoV-2 (right) while changing the relative infection rates for IAV and SARS-CoV-2. Yellow indicates either high peak viral loads or long infection durations, while dark blue indicates no infection.

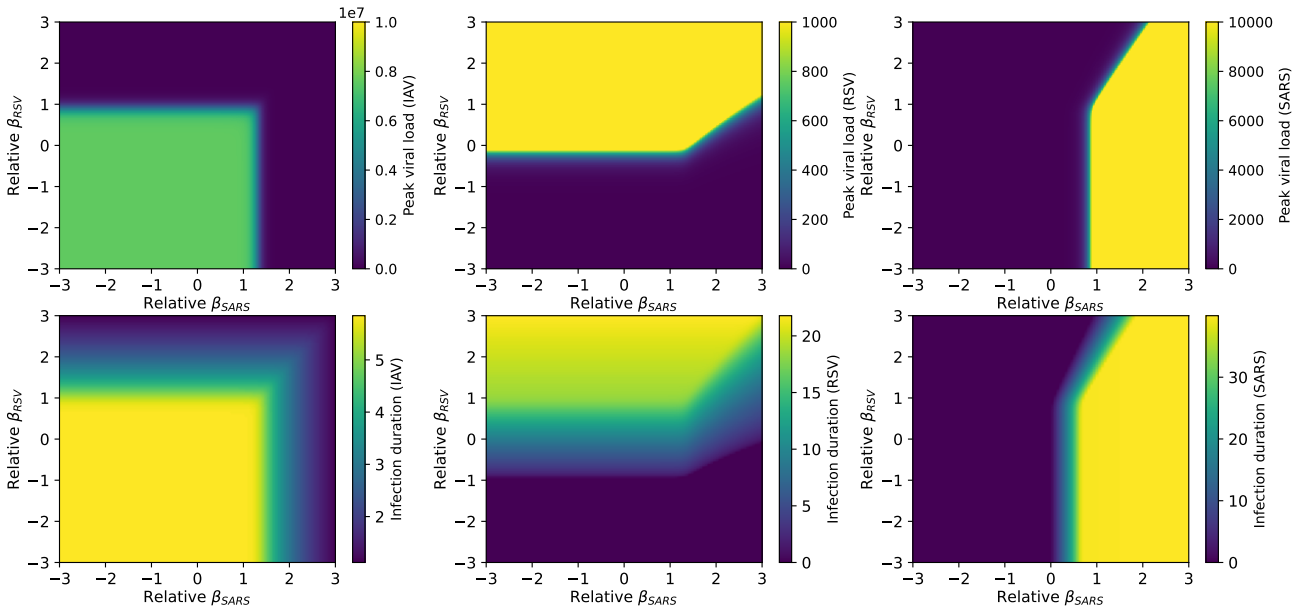


**Figure 5.** Peak viral load (top row) and infection duration (bottom row) for IAV (left), RSV (center), and SARS-CoV-2 (right) while changing the relative infection rates for RSV and SARS-CoV-2. Yellow indicates either high peak viral loads or long infection durations while dark blue indicates no infection.

SARS-CoV-2 infection rates become large enough to overcome the higher infection rate of IAV. Thus, a virus with a high infection rate is less likely to be suppressed by co-circulating viruses, even if those viruses are increasing in fitness.

Additionally, we note that there is a clear dependence of the threshold infection rate of one virus on the infection rates of the other two viruses. If there is no interaction among the viruses, then the threshold value of $\beta_c$ (Equation (3.2)) should not depend on the infection rates of the other viruses. As noted in the previous section, the viruses share target cells; therefore, as the infection rate of one virus increases, it infects target cells more rapidly; which leaves fewer target cells for other viruses and increases their threshold value of $\beta$. We can determine the relationship between the critical $\beta$ value of one virus and the infection rates of the others by incorporating the consumption of target cells into the expression for $\beta_c$. Note that competition for target cells is the only interaction between the viruses in our model; therefore, modifying $T_0$ is the only way to account for viral interactions when determining $\beta_c$. For each virus, the early viral growth dynamics are exponential and can be approximated by

$$V(t) = V_0 e^{\lambda_i t}, \tag{3.3}$$

where $\lambda_i$ is the growth rate of the $i^{th}$ virus as determined in [64]. Then, the target cells infected in the initial phase of infection is given by

$$\frac{dT}{dt} = -\sum_i \beta_i T V_{0i} e^{\lambda_i t}. \tag{3.4}$$

This can be integrated, which produces the following:

$$T(t) = T_0 \exp\left[\sum_i \frac{\beta_i V_{0i}}{\lambda_i} - \sum_i \frac{\beta_i V_{0i}}{\lambda_i} e^{\lambda_i t}\right]. \tag{3.5}$$

Putting this expression into the $R_0$-based threshold infection rate derived in the previous section (Equation (3.2)) gives a threshold value of the infection rate for IAV,

$$\beta_{c,\mathrm{IAV}} = \frac{c_{\mathrm{IAV}}\delta_{\mathrm{IAV}}}{p_{IAV}T_0} \exp\left[\sum_i \frac{\beta_i V_{0i}}{\lambda_i} e^{\lambda_i t} - \sum_i \frac{\beta_i V_{0i}}{\lambda_i}\right]. \tag{3.6}$$

The threshold values of RSV and SARS-CoV-2 infection rates have similar expressions. Figure 6 shows the threshold value of the IAV infection rate as a function of the RSV infection rate using this equation. Note that the predicted curve matches the threshold seen in Figure 3 (top left) quite well.

In addition to this minimum value of infection rate needed for an infection to grow, there is an upper boundary for growth of a particular virus, although those boundaries are determined by the infection rates of the other virus. This boundary occurs when the peak viral load of one virus reaches its maximum value. At this point, the peak viral loads of the other two viruses decline as a large number of target cells become infected by the first virus.

## 4. Discussion

We examined the dynamics of a triple virus respiratory tract infection consisting of IAV, RSV and SARS-CoV-2, which are three viruses that co-circulate and are capable of causing a tripledemic [5–7].

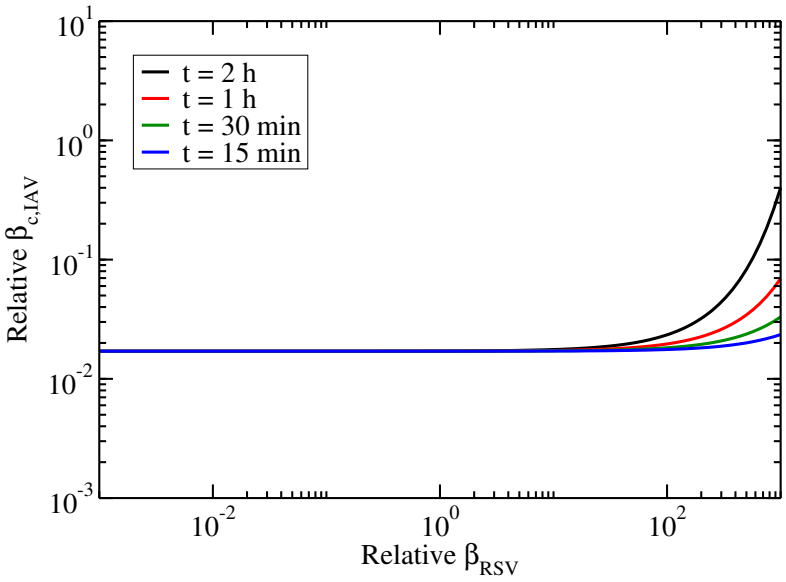


**Figure 6.** Threshold IAV infection rate to initiate IAV infections as a function of the RSV infection rate. Different colored lines indicate different assumed time periods.

We found that the presence of additional active viral infections affects the threshold infection rate needed to initiate an infection for a given virus. Additionally, we found that one virus can suppress the remaining two if the infection rate is such that the virus can infect more cells than the other two viruses. These findings suggest that the specific dynamics of a triple infection will change as these viruses mutate and strains with different infection rates arise [65, 66].

Experiments can help provide further insight into the dynamics of triple infections. The recent use of quantum dot probes can help track multiple viruses during a coinfection [67], thus providing insight into virus-virus interactions in vitro. There have been a number of recent studies that investigated coinfection with two respiratory viruses in animal models. However, there do not yet appear to be any studies of triple infections. While the percentage of patients with more than two viruses is small [1, 36–38], this constitutes an important group of patients who could potentially have medically complex outcomes if treatment does not include consideration of all infecting pathogens. Moreover, clinical treatment decisions could be complicated by low viral loads of a suppressed virus, thus potentially hampering our ability to detect the virus. Low viral loads were seen in this study for SARS-CoV-2, which is perhaps the most lethal of the three viruses [68–70].

Treatment strategies must address these unique circumstances. At least one clinical study examined the treatment of respiratory viral coinfections [71], although with only two viruses, and found that combination therapy worked better for co-infections than mono-therapy. An in vitro study examined the effectiveness of an antiviral that blocked the activity of sialyltransferases, and found that this was particularly helpful in co-infections of influenza and a common coronavirus [72]. Additionally, there was a mathematical modeling study of treatment of viral co-infections [73], which suggests that it is crucial to carefully consider the antiviral mechanism of action and dosage, as suboptimal treatment could either inadvertently prolong infections or unmask hidden co-infections, thus potentially worsening patient outcomes in the presence of respiratory viral co-infections. This effect was noted in an in vitro study of IAV and SARS-CoV-2, where treatment with oseltamivir reduced the IAV viral load and

allowed the SARS-CoV-2 viral loads to increase [31]. Our study suggests that the risk of this kind of outcome could be even worse when more than two viruses are involved. Our simulations show that one virus can suppress both of the other viruses involved in a triple infection; thus, treatment that only targets the dominant virus would allow for increased replication of the other two viruses.

The model has limitations that could affect its accuracy in simulating triple infections. One simplification is a lack of explicit immune response dynamics, particularly the innate immune response, which plays a crucial role in virus-virus interactions [27,30,56,74]. Moreover, it does not fully capture other essential viral interaction mechanisms such as super-infection [55], target cell partitioning [75], and super-infection exclusion [76, 77], thus potentially oversimplifying the complex dynamics of co-infection. Additionally, we neglected cell regeneration, which could alter particularly long-term viral dynamics [54,55], thus affecting our ability to assess whether triple infections can result in long-lasting or chronic infections. Incorporating these factors could significantly enhance the model's predictions and provide a more realistic understanding of viral infections.

Additionally, stochastic effects — random variations inherent in biological systems due to the unpredictability of biological processes and the discrete nature of individuals and viral particles — can alter model predictions [78]. Stochastic effects can lead to notable fluctuations in the viral load and immune responses, particularly in smaller populations or during the early stages of infection, thus potentially allowing a virus that would typically be suppressed to instead take hold and have more of a role in the viral time course. By accounting for these stochastic elements, a model would better reflect the real-world complexities of viral dynamics, especially in coinfection scenarios where interactions between different pathogens introduce additional layers of variability. Finally, ordinary differential equation (ODE) models neglect spatial effects, which could also play a role in the dynamics of triple infections. Different viruses will have different diffusion coefficients [79], and will disperse through the respiratory tract at different rates. Spatial effects could be taken into account through the use of an agent-based model [80] that explicitly models a layer of cells with virus moving over the surface.

## 5. Conclusion

While the model developed here is fairly simple and should not be used to make specific viral load predictions, it gives us insight into the interactions of multiple viruses during a coinfection. We found that changes in the infection rate of a virus could allow it to suppress other viruses during the coinfection. The development of more comprehensive models would ultimately improve our understanding of how viruses behave under fluctuating conditions, thereby informing more effective public health strategies.

## Author contributions

Conceptualization, HMD; Data curation, SS; Formal analysis, SS; Investigation, SS; Methodology, SS and HMD; Project administration, HMD; Software, SS; Supervision, HMD; Validation, SS and HMD; Visualization, SS; Writing – original draft, SS; Writing – review & editing, HMD.

## Use of AI tools declaration

The authors declare they have not used Artificial Intelligence (AI) tools in the creation of this article.

## Conflict of interest

The authors have no conflicts of interest to declare.

## References


1. G. Shirreff, S. S. Chaves, L. Coudeville, B. Mengual-Chulia, A. Mira-Iglesias, J. Puig-Barbera, et al., Seasonality and co-detection of respiratory viral infections among hospitalised patients admitted with acute respiratory illness-Valencia region, Spain, 2010–2021, *Influenza Other Respi. Viruses*, **18** (2024), e70017. https://doi.org/10.1111/irv.70017
2. N. C. Marshall, R. M. Kariyawasam, N. Zelyas, J. N. Kanji, M. A. Diggle, Broad respiratory testing to identify sars-cov-2 viral co-circulation and inform diagnostic stewardship in the COVID-19 pandemic, *Virol. J.*, **18** (2021), 93. https://doi.org/10.1186/s12985-021-01545-9
3. S. Nickbakhsh, F. Thorburn, B. Von Wissmann, J. McMenamin, R. N. Gunson, P. R. Murcia, Extensive multiplex PCR diagnostics reveal new insights into the epidemiology of viral respiratory infections, *Epidemiol. Infect.*, **144** (2016), 2064–2076. https://doi.org/10.1017/S0950268816000339
4. G. Guido, E. Lalle, S. Mosti, P. Mencarini, D. Lapa, R. Libertone, et al., Recovery from triple infection with SARS-CoV-2, RSV and influenza virus: A case report, *J. Infect. Public Health*, **16** (2023), 1045–1047. https://doi.org/10.1016/j.jiph.2023.05.001
5. M. K. Lee, D. Alfego, S. E. Dale, Prevalence and trends in mono- and co-infection of COVID-19, influenza A/B, and respiratory syncytial virus, January 2018–June 2023, *Front. Public Health*, **11** (2023), 1297981. https://doi.org/10.3389/fpubh.2023.1297981
6. A. H. Baker, L. K. Lee, B. E. Sard, S. Chung, The 4 S's of disaster management framework: A case study of the 2022 pediatric tripledemic response in a community hospital, *Ann. Emerg. Med.*, **83** (2024), 568–575. https://doi.org/10.1016/j.annemergmed.2024.01.020
7. W. Luo, Q. Liu, Y. Zhou, Y. Ran, Z. Liu, W. Hou, et al., Spatiotemporal variations of "triple-demic" outbreaks of respiratory infections in the united states in the post COVID-19 era, *BMC Public Health*, **23** (2023), 2452. https://doi.org/10.1186/s12889-023-17406-9
8. E. R. Tavares, T. F. de Lima, G. Bartolomeu-Goncalves, I. M. de Castro, D. G. de Lima, P. H. G. Borges, et al., Development of a melting-curve-based multiplex real-time PCR assay for the simultaneous detection of viruses causing respiratory infection, *Microorganisms*, **11** (2023), 2692. https://doi.org/10.3390/microorganisms11112692
9. R. Cohen, H. Haas, O. Romain, S. Bechet, C. Romain, C. D. T. de Lays, et al., Use of rapid antigen triple test nasal swabs (COVID-VIRO ALL-IN TRIPLEX: Severe acute respiratory syndrome coronavirus 2, respiratory syncytial virus, and influenza) in children with respiratory symptoms: A real-life prospective study, *Open Forum Infect Diseases*, **11** (2024), ofad617. https://doi.org/10.1093/ofid/ofad617

10.F. Ahmadi, F. Z. Zanganeh, I. A. Tehrani, S. Shoaee, H. Choobin, A. Bozorg, et al., Evaluating an extraction-free sample preparation method for multiplex detection of SARS-Cov-2, influenza A/B, and RSV with implementation on a microfluidic chip, *Diagn. Microbiol. Infect. Disease*, **109** (2024), 116325. https://doi.org/10.1016/j.diagmicrobio.2024.116325

11.T. Y. Kim, G. E. Bae, J.-Y. Kim, M. Kang, J.-H. Jang, H. J. Huh, et al., Evaluation of the Kaira COVID-19/flu/rsv detection kit for detection of SARS-CoV-2, influenza A/B, and respiratory syncytial virus: A comparative study with the PowerChek SARS-CoV-2, influenza A&B, RSV multiplex real-time PCR kit, *PLoS One*, **17** (2022), e0278530. https://doi.org/10.1371/journal.pone.0278530

12.N. Sultanoglu, E. Erdag, C. S. Ozverel, A single antiviral for a triple epidemic: Is it possible?, *Future Virol.*, **18** (2023), 633–642. https://doi.org/10.2217/fvl-2023-0048

13.Y. Wang, X. Wei, Y. Liu, S. Li, W. Pan, J. Dai, et al., Towards broad-spectrum protection: the development and challenges of combined respiratory virus vaccines, *Front. Cellular Infect. Microbiol.*, **14** (2024), 1412478. https://doi.org/10.3389/fcimb.2024.1412478

14.L. Pinky, H. M. Dobrovolny, Coinfections of the respiratory tract: Viral competition for resources, *PLoS ONE*, **11** (2016), e0155589. https://doi.org/10.1371/journal.pone.0155589

15.A. Pizzorno, B. Padey, V. Duliere, W. Mouton, J. Oliva, E. Laurent, et al., Interactions between severe acute respiratory syndrome coronavirus 2 replication and major respiratory viruses in human nasal epithelium, *J. Infect. Diseases*, **226** (2022), 2095–2104. https://doi.org/10.1093/infdis/jiac357

16.N. Sankuntaw, N. Punyadee, W. Chantratita, V. Lulitanond, Coinfection with respiratory syncytial virus and rhinovirus increases IFN-$\lambda$1 and CXCL10 expression in human primary bronchial epithelial cells, *New Microbiol.*, **47** (2024), 60–67.

17.E.-H. Kim, T.-Q. Nguyen, M. A. B. Casel, R. Rollon, S.-M. Kim, Y.-I. Kim, et al., Coinfection with SARS-CoV-2 and influenza A virus increases disease severity and impairs neutralizing antibody and CD4+ T cell responses, *J. Virol.*, **96** (2022), e01873-21. https://doi.org/10.1128/jvi.01873-21

18.G. Cox, A. J. Gonzalez, E. C. Ijezie, A. Rodriguez, C. R. Miller, J. T. Van Leuven, et al., Priming with rhinovirus protects mice against a lethal pulmonary coronavirus infection, *Front. Immunol.*, **13** (2022), 886611. https://doi.org/10.3389/fimmu.2022.886611

19.K. Trepat, A. Gibeaud, S. Trouillet-Assant, O. Terrier, Exploring viral respiratory coinfections: Shedding light on pathogen interactions, *PLoS Pathogens*, **20** (2024), e1012556. https://doi.org/10.1371/journal.ppat.1012556

20.M. J. Kim, S. Kim, H. Kim, D. Gil, H.-J. Han, R. K. Thimmulappa, et al., Reciprocal enhancement of SARS-CoV-2 and influenza virus replication in human pluripotent stem cell-derived lung organoids, *Emerg. Microb. Infect.*, **12** (2023), 2211685. https://doi.org/10.1080/22221751.2023.2211685

21.J. J. Clark, R. Penrice-Randal, P. Sharma, X. Dong, S. H. Pennington, A. E. Marriott, et al., Sequential infection with influenza a virus followed by severe acute respiratory syndrome coronavirus 2 (SARS-CoV-2) leads to more severe disease and encephalitis in a mouse model of COVID-19, *Viruses—Basel*, **16** (2024), 863. https://doi.org/10.3390/v16060863

22.K. Roe, Lethal synergistic infections by two concurrent respiratory pathogens, *Arch. Med. Res.*, **56** (2024), 103101. https://doi.org/10.1016/j.arcmed.2024.103101

23. K. F. Chan, L. A. Carolan, D. Korenkov, J. Druce, J. McCaw, P. C. Reading, et al., Investigating viral interference between influenza A virus and human respiratory syncytial virus in a ferret model of infection, *J. Infect. Dis.*, **218** (2018), 406–417. https://doi.org/10.1093/infdis/jiy184

24. Y. Drori, J. Jacob-Hirsch, R. Pando, A. Glatman-Freedman, N. Friedman, E. Mendelson, et al., Influenza A virus inhibits RSV infection via a two-wave expression of IFIT proteins, *Viruses — Basel*, **12** (2020), 1171. https://doi.org/10.3390/v12101171

25. M. Shinjoh, K. Omoe, N. Saito, N. Matsuo, K. Nerome, In vitro growth profiles of respiratory syncytial virus in the presence of influenza virus, *Acta Virol.*, **44** (2000), 91–97.

26. S. M. Hartwig, A. M. Miller, S. M. Varga, Respiratory syncytial virus provides protection against a subsequent influenza A virus infection, *J. Immunol.*, **208** (2022), 1–12. https://doi.org/10.4049/jimmunol.2000751

27. M. Czerkies, M. Kochanczyk, Z. Korwek, W. Prus, T. Lipniacki, Respiratory syncytial virus protects bystander cells against influenza A virus infection by triggering secretion of type I and type III interferons, *J. Virol.*, **96** (2022), e01341-22. https://doi.org/10.1128/jvi.01341-22

28. S. M. Hartwig, A. Odle, L.-Y. R. Wong, D. K. Meyerholz, S. Perlman, S. M. Varga, Respiratory syncytial virus infection provides protection against severe acute respiratory syndrome coronavirus challenge, *J. Virol.*, **98** (2024), e00669-24. https://doi.org/10.1128/jvi.00669-24

29. K. Dee, V. Schultz, J. Haney, L. A. Bissett, C. Magill, P. R. Murcia, Influenza A and respiratory syncytial virus trigger a cellular response that blocks severe acute respiratory syndrome virus 2 infection in the respiratory tract, *J. Infect. Diseases*, **227** (2023), 1396–1406. https://doi.org/10.1093/infdis/jiac494

30. S. Gilbert-Girard, J. Piret, J. Carbonneau, M. Henaut, N. Goyette, G. Boivin, Viral interference between severe acute respiratory syndrome coronavirus 2 and influenza A viruses, *PLoS Pathogens*, **20** (2024), e1012017. https://doi.org/10.1371/journal.ppat.1012017

31. N. R. Cheemarla, T. A. Watkins, V. T. Mihaylova, E. F. Foxman, Viral interference during influenza A-SARS-CoV-2 coinfection of the human airway epithelium and reversal by oseltamivir, *J. Infect. Diseases*, **229** (2024), 1430-–1434. https://doi.org/10.1093/infdis/jiad402

32. K. Oishi, S. Horiuchi, J. M. Minkoff, B. R. tenOever, The host response to influenza A virus interferes with SARS-CoV-2 replication during coinfection, *J. Virol.*, **96** (2022), e00765-22. https://doi.org/10.1128/jvi.00765-22

33. H. C. Maltezou, A. Papanikolopoulou, S. Vassiliu, K. Theodoridou, G. Nikolopoulou, N. V. Sipsas, COVID-19 and respiratory virus co-infections: A systematic review of the literature, *Viruses — Basel*, **15** (2023), 865. https://doi.org/10.3390/v15040865

34. E. A. Goka, P. J. Vallely, K. J. Mutton, P. E. Klapper, Single, dual and multiple respiratory virus infections and risk of hospitalization and mortality, *Epidemiol. Infect.*, **143** (2015), 37–47. https://doi.org/10.1017/S0950268814000302

35. P. I. Babawale, A. Guerrero-Plata, Respiratory viral coinfections: Insights into epidemiology, immune response, pathology, and clinical outcomes, *Pathogens*, **13** (2024), 316. https://doi.org/10.3390/pathogens13040316

36. H. Al Kindi, L. W. Meredith, A. Al-Jardani, F. Sajina, I. Al Shukri, R. al Haj, et al., Time trend of respiratory viruses before and during the COVID-19 pandemic in severe acute respiratory virus infection in the Sultanate of Oman between 2017 and 2022, *Influenza Other Respi. Viruses*, **17** (2023), e13233. https://doi.org/10.1111/irv.13233

37. C. Mantelli, P. Colson, L. Lesage, D. Stoupan, H. Chaudet, A. Morand, et al., Coinfections and iterative detection of respiratory viruses among 17,689 patients between March 2021 and December 2022 in Southern France, *J. Clin. Virol.*, **175** (2024), 105744. https://doi.org/10.1016/j.jcv.2024.105744

38. B. Nieto-Rivera, Z. Saldana-Ahuactzi, I. Parra-Ortega, A. Flores-Alanis, E. Carbajal-Franco, A. Cruz-Rangel, et al., Frequency of respiratory virus-associated infection among children and adolescents from a tertiary-care hospital in Mexico City, *Sci. Rep.*, **13** (2023), 19763. https://doi.org/10.1038/s41598-023-47035-6

39. H. M. Dobrovolny, How do viruses get around? a review of mathematical modeling of in-host viral transmission, *Virology*, **604** (2025), 110444. https://doi.org/10.1016/j.virol.2025.110444

40. E. Mochan, T. J. Sego, Mathematical modeling of the lethal synergism of coinfecting pathogens in respiratory viral infections: A review, *Microorganisms*, **11** (2023), 2974. https://doi.org/10.3390/microorganisms11122974

41. J. Yin, J. Redovich, Kinetic modeling of virus growth in cells, *Microbiol. Mol. Biol. Rev.*, **82** (2018), e00066–17. https://doi.org/10.1128/MMBR.00066-17

42. M. Zhang, M. Li, J. Ma, The role of long-lived plasma cells in viral clearance, *J. Biol. Dynam.*, **18** (2024). https://doi.org/10.1080/17513758.2024.2325523

43. M. W. Tan, A. J. N. Anelone, A. T. Tay, R. Y. Tan, K. Zeng, K. B. Tan, et al., Differences in virus and immune dynamics for SARS-CoV-2 delta and omicron infections by age and vaccination histories, *BMC Infect. Diseases*, **24** (2024). https://doi.org/10.1186/s12879-024-09572-x

44. D. Stocks, A. Thomas, A. Finn, L. Danon, E. Brooks-Pollock, Mechanistic models of humoral kinetics following COVID-19 vaccination, *J. Royal Soc. Interface*, **22** (2024). https://doi.org/10.1098/rsif.2024.0445

45. A. Suri, S. Satani, H. M. Dobrovolny, Analyzing differences in viral dynamics between vaccinated and unvaccinated RSV patients, *Epedemiologia*, **6** (2025), 16. https://doi.org/10.3390/epidemiologia6020016

46. L. Schuh, P. V. Markov, I. Voulgaridi, Z. Bogogiannidou, V. A. Mouchtouri, C. Hadjichristodoulou, et al., Within-host dynamics of antiviral treatment with remdesivir for SARS-CoV-2 infection, *J. Royal Soc. Interface*, **21** (2024). https://doi.org/10.1098/rsif.2024.0536

47. A. Chiarelli, H. Dobrovolny, Viral rebound after antiviral treatment: A mathematical modeling study of the role of antiviral mechanism of action, *Interdiscipl. Sci. Comput. Life Sci.*, **16** (2024), 844–853. https://doi.org/10.1007/s12539-024-00643-w

48. T. Phan, R. M. Ribeiro, G. E. Edelstein, J. Boucau, R. Uddin, C. Marino, et al., Modeling suggests SARS-CoV-2 rebound after nirmatrelvir-ritonavir treatment is driven by target cell preservation coupled with incomplete viral clearance, *J. Virol.*, **99** (2025), e01623-24. https://doi.org/10.1128/jvi.01623-24

49. B. Jessie, H. Dobrovolny, The role of syncytia during viral infections, *J. Theor. Biol.*, **525** (2021), 110749. https://doi.org/10.1016/j.jtbi.2021.110749

50. Z. Noffel, H. M. Dobrovolny, Quantifying the effect of defective viral genomes in respiratory syncytial virus infections, *Math. Biosci. Eng.*, **20** (2023), 12666–12681. https://doi.org/10.3934/mbe.2023564

51. L. Schuh, P. Markov V, V. M. Veliov, N. I. Stilianakis, A mathematical model for the within-host (re)infection dynamics of SARS-CoV-2, *Math. Biosci.*, **371** (2024), 109178. https://doi.org/10.1016/j.mbs.2024.109178

52. B. Fain, H. M. Dobrovolny, Initial inoculum and the severity of COVID-19: A mathematical modeling study of the dose-response of SARS-CoV-2 infections, *Epidemiologia*, **1** (2020), 5–15. https://doi.org/10.3390/epidemiologia1010003

53. L. Pinky, J. R. DeAguero, C. H. Remien, A. M. Smith, How interactions during viral-viral coinfection can shape infection kinetics, *Viruses-Basel*, **15** (2023), 1303. https://doi.org/10.3390/v15061303

54. L. Pinky, H. M. Dobrovolny, The impact of cell regeneration on the dynamics of viral coinfection, *Chaos*, **27** (2017), 063109. https://doi.org/10.1063/1.4985276

55. L. Pinky, G. González-Parra, H. M. Dobrovolny, Superinfection and cell regeneration can lead to chronic viral coinfections, *J. Theor. Biol.*, **466** (2019), 24–38. https://doi.org/10.1016/j.jtbi.2019.01.011

56. Z. Noffel, H. M. Dobrovolny, Modeling the bystander effect during viral coinfection, *J. Theor. Biol.*, **594** (2024), 111928. https://doi.org/10.1016/j.jtbi.2024.111928

57. N. Polavarapu, M. Doty, H. M. Dobrovolny, Exploring the treatment of SARS-CoV-2 with modified vesicular stomatitis virus, *J. Theor. Biol.*, **595** (2024), 111959. https://doi.org/10.1016/j.jtbi.2024.111959

58. M. A. Taye, Host viral load during triple coinfection of SARS-CoV-2, influenza virus, and syncytial virus, *Contempor. Msth.*, **4** (2023), 392–410. https://doi.org/10.37256/cm.4320232500

59. Y. Lu, T. Zhao, M. Lu, Y. Zhang, X. Yao, G. Wu, et al., The analyses of high infectivity mechanism of sars-cov-2 and its variants, *COVID*, **1** (2021), 666–673. https://doi.org/10.3390/covid1040054

60. H. Choi, P. Chatterjee, M. Hwang, E. Lichtfouse, V. K. Sharma, C. Jinadatha, The viral phoenix: enhanced infectivity and immunity evasion of SARS-CoV-2 variants, *Environm. Chem. Lett.*, **20** (2022), 1539–1544. https://doi.org/10.1007/s10311-021-01318-4

61. Y. Hu, S. Peng, B. Su, T. Wang, J. Lin, W. Sun, et al., Laboratory studies on the infectivity of human respiratory viruses: Experimental conditions, detections, and resistance to the atmospheric environment, *Fund. Res.*, **4** (2024), 471–483. https://doi.org/10.1016/j.fmre.2023.12.017

62. T. C. Bouton, J. Atarere, J. Turcinovic, S. Seitz, C. Sher-Jan, M. Gilbert, et al., Viral dynamics of omicron and delta severe acute respiratory syndrome coronavirus 2 (SARS-CoV-2) variants with implications for timing of release from isolation: A longitudinal cohort study, *Clin. Infect. Diseases*, **76** (2023), E227–E233. https://doi.org/10.1093/cid/ciac510

63. L. Pinky, H. M. Dobrovolny, SARS-CoV-2 coinfections: Could influenza and the common cold be beneficial?, *J Med Virol.*, **92** (2020), 2623–2630. https://doi.org/10.1002/jmv.26098

64. A. M. Smith, F. R. Adler, A. S. Perelson, An accurate two-phase approximate solution to an acute viral infection model, *J. Math. Biol.*, **60** (2010), 711–726. https://doi.org/10.1007/s00285-009-0281-8

65. L. Xue, S. Jing, K. Zhang, R. Milne, H. Wang, Infectivity versus fatality of SARS-CoV-2 mutations and influenza, *Int. J. Infect. Diseases*, **121** (2022), 195–202. https://doi.org/10.1016/j.ijid.2022.05.031

66. D. Niemeyer, S. Stenzel, T. Veith, S. Schroeder, K. Friedmann, F. Weege, et al., SARS-CoV-2 variant alpha has a spike-dependent replication advantage over the ancestral B.1 strain in human cells with low ACE2 expression, *PLoS Biol.*, **20** (2022), e3001871. https://doi.org/10.1371/journal.pbio.3001871

67. T. K. Fayyadh, F. Ma, C. Qin, X. Zhang, W. Li, X.-E. Zhang, et al., Simultaneous detection of multiple viruses in their co-infected cells using multicolour imaging with self-assembled quantum dot probes, *Microch. Acta*, **184** (2017), 2815–2824. https://doi.org/10.1007/s00604-017-2300-6

68. L. E. Wee, J. T. Lim, R. W. L. Ho, C. J. Chiew, B. Young, I. Venkatachalam, et al., Severity of respiratory syncytial virus versus SARS-CoV-2 omicron and influenza infection amongst hospitalized singaporean adults: A national cohort study, *Lancet Regional Health—Western Pacific*, **55** (2025), 101494. https://doi.org/10.1016/j.lanwpc.2025.101494

69. K. L. Bajema, D. P. Bui, L. Yan, Y. Li, N. Rajeevan, R. Vergun, et al., Severity and long-term mortality of COVID-19, influenza, and respiratory syncytial virus, *JAMA Int. Med.*, **185** (2025), 324–334. https://doi.org/10.1001/jamainternmed.2024.7452

70. S. Khanal, B. Khanal, F.-S. Chou, A. J. Moon-Grady, L. V. Ghimire, Comparison of mortality and cardiovascular complications due to COVID-19, RSV, and influenza in hospitalized children and young adults, *BMC Cardiovac. Disord.*, **24** (2024), 686. https://doi.org/10.1186/s12872-024-04366-0

71. D. Liu, K.-Y. Leung, H.-Y. Lam, R. Zhang, Y. Fan, X. Xie, et al., Interaction and antiviral treatment of coinfection between SARS-CoV-2 and influenza in vitro, *Virus Res.*, **345** (2024), 199371. https://doi.org/10.1016/j.virusres.2024.199371

72. M. R. Amin, K. N. Anwar, M. J. Ashraf, M. Ghassemi, R. M. Novak, Preventing human influenza and coronaviral mono or coinfection by blocking virus-induced sialylation, *Antiviral Res.*, **232** (2024), 106041. https://doi.org/10.1016/j.antiviral.2024.106041

73. P. Alexander, H. M. Dobrovolny, Treatment of respiratory viral coinfections, *Epidemiologia*, **3** (2022), 81–96. https://doi.org/10.3390/epidemiologia3010008

74. M. Essaidi-Laziosi, J. Geiser, S. Huang, S. Constant, L. Kaiser, C. Tapparel, Interferon-dependent and respiratory virus-specific interference in dual infections of airway epithelia, *Sci. Rep.*, **10** (2020), 10246. https://doi.org/10.1038/s41598-020-66748-6

75. L. Pinky, H. M. Dobrovolny, Epidemiological consequences of viral interference: A mathematical modeling study of two interacting viruses, *Front. Microbiol.*, **13** (2022), 830423. https://doi.org/10.3389/fmicb.2022.830423

76. J. Biryukov, C. Meyers, Superinfection exclusion between two high-risk human papillomavirus types during a coinfection, *J. Virol.*, **92** (2018), 01993-17. https://doi.org/10.1128/JVI.01993-17

77.A. Sims, L. B. Tornaletti, S. Jasim, C. Pirillo, R. Devlin, J. C. Hirst, et al., Superinfection exclusion creates spatially distinct influenza virus populations, *PLoS Biol.*, **21** (2023), e3001941. https://doi.org/10.1371/journal.pbio.3001941

78.L. Pinky, G. Gonzalez-Parra, H. M. Dobrovolny, Effect of stochasticity on coinfection dynamics of respiratory viruses, *BMC Bioinform.*, **20** (2019), 191. https://doi.org/10.1186/s12859-019-2793-6

79.R. Cush, P. Russo, Z. Kucukyavuz, Z. Bu, D. Neau, D. Shih, et al., Rotational and translational diffusion of a rodlike virus in random coil polymer solutions, *Macromolecules*, **30** (1997), 4920–4926. https://doi.org/10.1021/ma970032f

80.B. Fain, H. M. Dobrovolny, GPU acceleration and data fitting: Agent-based models of viral infections can now be parameterized in hours, *J. Comp. Sci.*, **61** (2022), 101662. https://doi.org/10.1016/j.jocs.2022.101662


AIMS Press